Achievable high V_{oc} of carbon based all-inorganic $CsPbIBr_2$ perovskite solar cells through interface engineering

Zhanglin Guo, Siowhwa Teo, Zhenhua Xu, Chu Zhang, Yusuke Kamata, Shuzi Hayase, Tingli Ma*

Graduate School of Life Science and Systems Engineering, Kyushu Institute of Technology, Kitakyushu, Fukuoka 808-0196, Japan
*(*Corresponding author: tinglima@life.kyutech.ac.jp)*

Experimental Section

Materials: Caesium iodide (CsI, 99.9%), dimethyl sulfoxide (DMSO) were purchased from Sigma-Aldrich. Lead bromide ($PbBr_2$) was purchased from TCI. SnO_2 colloid (tin (IV) oxide) precursor was purchased from Alfa Aesar. SnCl2 (99.9%) was purchased from Wako. The ITO-coated glass was purchased from Yingkou OPV Tech Co., Ltd. The conductive carbon paste was purchased from Ningbo Borun New Material Technology Co., Ltd.

Device Fabrication: The 1.0 M $CsPbIBr_2$ perovskite precursor was prepared by dissolving the CsI and $PbBr_2$ in DMSO with the mole ratio of 1/1, then stirring at 60 ^oC until the clear solution was obtained. The ITO-coated glass (Yingkou OPV Tech Co., Ltd) was used as substrate cathode and the surface was washed successively with ultrapure water, acetone, isopropanol and ethanol in an ultrasonic cleaner. The dried ITO substrates were treated in UV-Ozone cleaner for 20 min. The SnO_2 colloid precursor (Alfa Aesar, 15% in H_2O colloidal dispersion) was diluted by H_2O to 2.67% and was spin coated onto ITO/glass substrates at 2000 rpm for 30 s, and then baked on a hot plate in ambient air at 150 ^oC for 30 min. Then $SnCl_2$ solution (the concentration varies from 0.05 M to 0.15 M) was deposited on the SnO_2 nanoparticles film (NPs) and baked at 100 ^oC for 10min and 180 ^oC for 1 hour. Subsequently, in the nitrogen-filled glove box, the perovskite precursor solution was deposited on the SnO_2 layer via a spin-coating program at 1000 rpm for 10s and then 3000 rpm for 30 s. After the spin-coating process, the obtained film was placed for 5 min and then annealed at 160 ^oC for 10 min on a hot plate in the glove box. For completing the device, the carbon electrode was deposited on the top of the $CsPbIBr_2$ film by doctor-blading technology using scotch tape to control the electrode thickness. Then the cells were heated treated at 100 °C for 10 min in ambient conditions to promote evaporation of residual solvents.

Characteristics: The X-ray diffracting (XRD) patterns were recorded from 5 ° to 50 ° at a scanning step of 0.01^o s^{-1} using X-ray diffractometer (Rigaku Co. Ltd., Tokyo, Japan) with Cu Kα radiation (λ=1. 54056 Å). The field emission scanning electron microscope (FE-SEM) (JSM-6701, JEOL) was used to characterize the morphology of the films. The AFM images were measured by Surface Probe Microscopy (SPM, JSPM-5200, JEOL). A UV-VIS-NIR spectrophotometer (V-670, JASSCO Co. Ltd., USA) was applied to characterize the optical properties of the samples. The electrochemical impedance spectroscopy (EIS) was measured by the Solartron Analytical 1255B. The *J-V* curves of the devices were measured by Keithley 2450 interfaced with a xenon lamp (Bunko Keiki BSOX150LC) at 100 mW cm^{-2} under AM 1.5G conditions. The power of the light exposure from the solar simulator was fixed with an amorphous Si photodetector (Bunko Keiki BS-520 S/N 353). The IPCE were measured by monochromatic illumination (A 300 W Xenon arc lamp through Nikon G250 monochromator equipped). The transient photovoltage

decay measurements were carried out using a 630-nm diode laser (without a background light bias) with the 5ns pulse duration and 4 Hz pulse frequency. The voltage responses from the device were recorded using an Iwatsu digital oscilloscope DS-5554. The cell area was precisely controlled using a 0.08 cm^2 black metal mask to measure the photovoltaic performance of the devices.

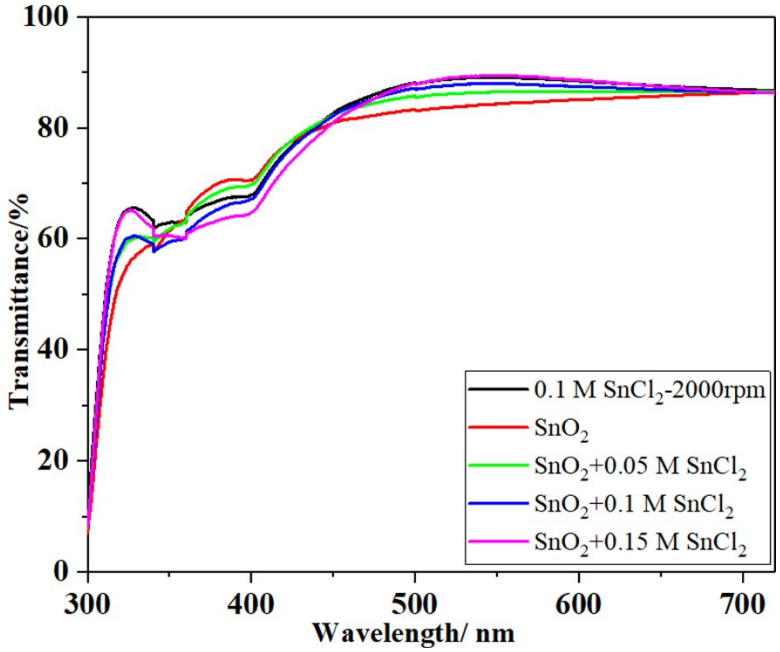

Figure S1 Transmission spectra of different SnO_2 films on ITO substrate.

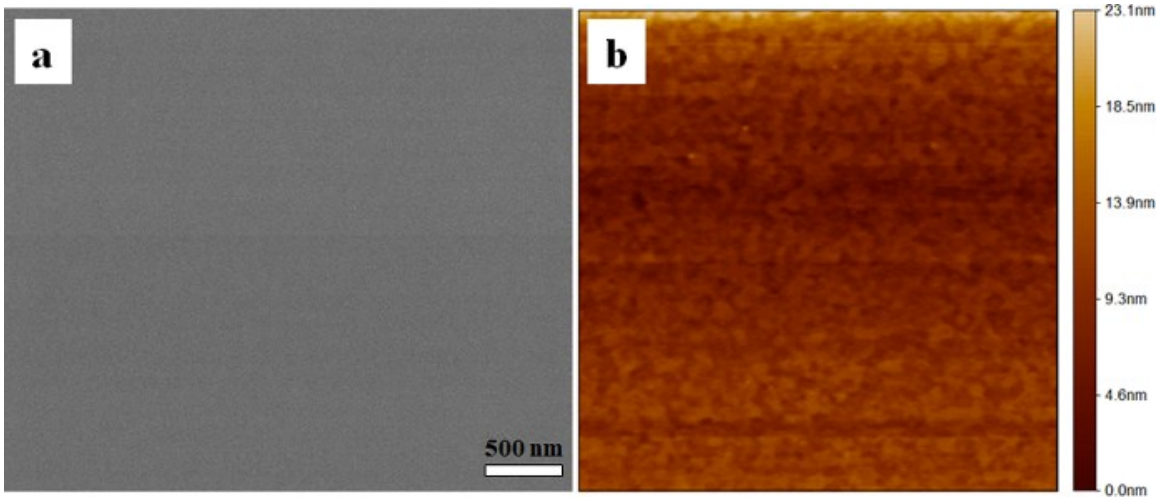

Figure S2 (a) SEM and (b) AFM image of SnO_2 film passivated with 0.15 M $SnCl_2$ solution.

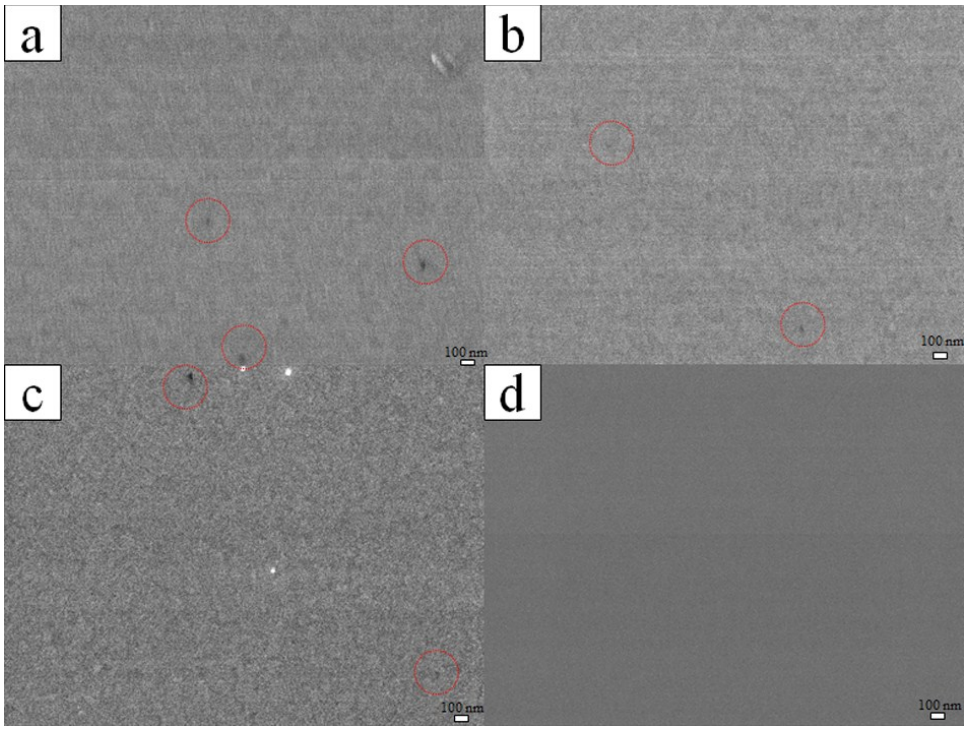

Figure S3 SEM images of SnO_2 nanocrystal films: (a) annealed at 150 °C for 30 min, (b) annealed at 150 °C for 30 min and then 180 °C for 1 h, (c) annealed at 180 °C for 1 h; and (d) $SnCl_2$ passivated film annealed at 180 °C for 1 h.

We conducted the control experiments to confirm the effect of 180 °C annealing on the roughness of the resultant SnO_2 nanocrystal films. The spin-coated SnO_2 nanocrystal films with different annealing processes are shown in Figure S3. We can find that there is no obvious difference for annealing at 180 °C for 1 h after annealing at 150 °C for 30 min. While directly annealing the spin-coated SnO_2 nanocrystal film at 180 °C for 1 h results a rougher film, which might be attributed to that higher annealing temperature will lead to aggregation of the nanocrystals. While after passivation using $SnCl_2$-ethanol solution, a much smoother film can be obtained (Figure S3d). Thus the 180 °C annealing is not the decisive factor for getting smooth SnO_2 film.

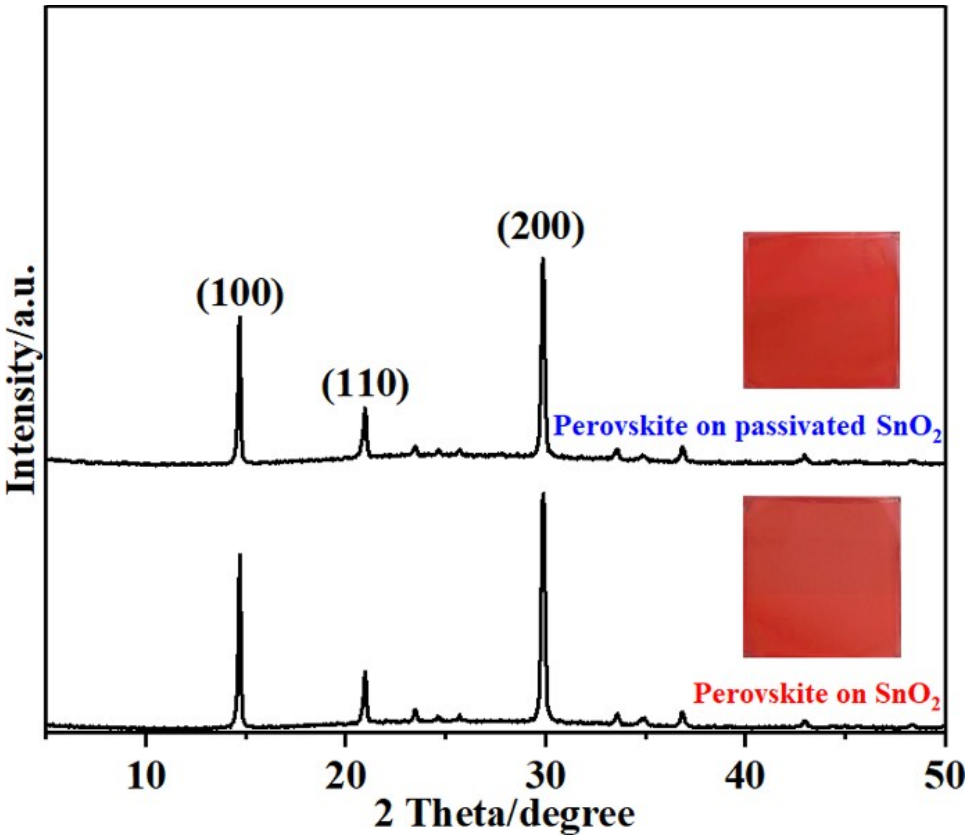

Figure S4 XRD patterns of $CsPbIBr_2$ perovskite film deposited on bare or passivated SnO_2 ESL. Inset: photographs of the respective perovskite film.

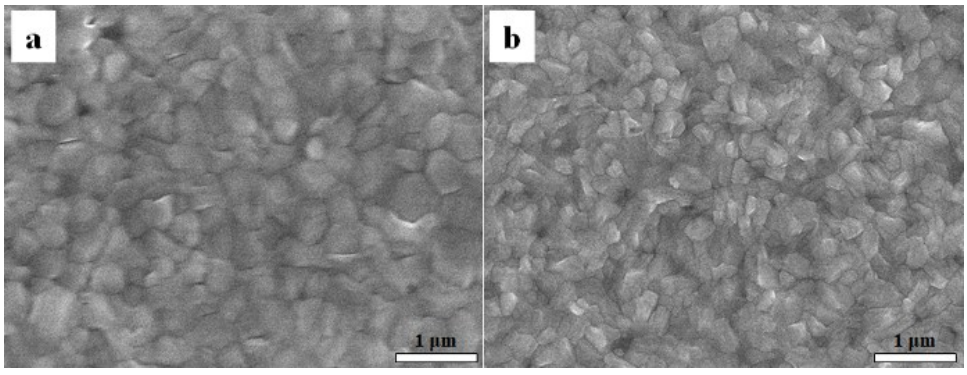

Figure S5 SEM images of $CsPbIBr_2$ perovskite film deposited on bare or passivated SnO_2 ESL.

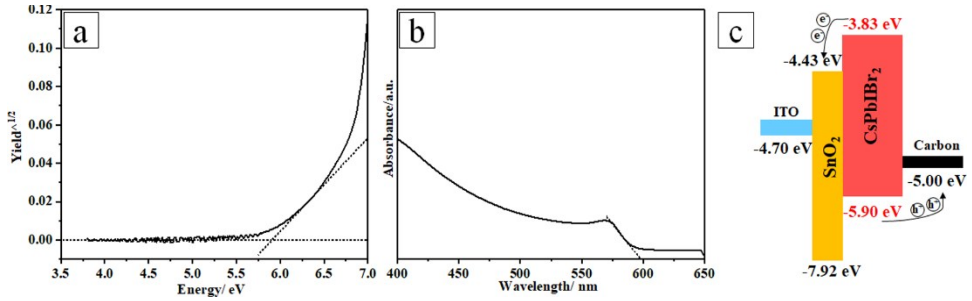

Figure S6 (a) The photoelectron yield spectroscopy, (b) UV-vis spectrum of $CsPbIBr_2$ film and (c) the energy levels of the components.

From **Fig. S6a**, we can see that the valence band of $CsPbIBr_2$ is -5.90 eV. **Fig. S6b** indicates that the absorption band edge is about 598 nm, thus the band gap of $CsPbIBr_2$ is 2.07 eV. From these two spectra, the energy level of the perovskite material can be depicted as **Fig. S6c**, where the SnO_2 ESL can effectively transfer the photo-generated electrons and block the holes.

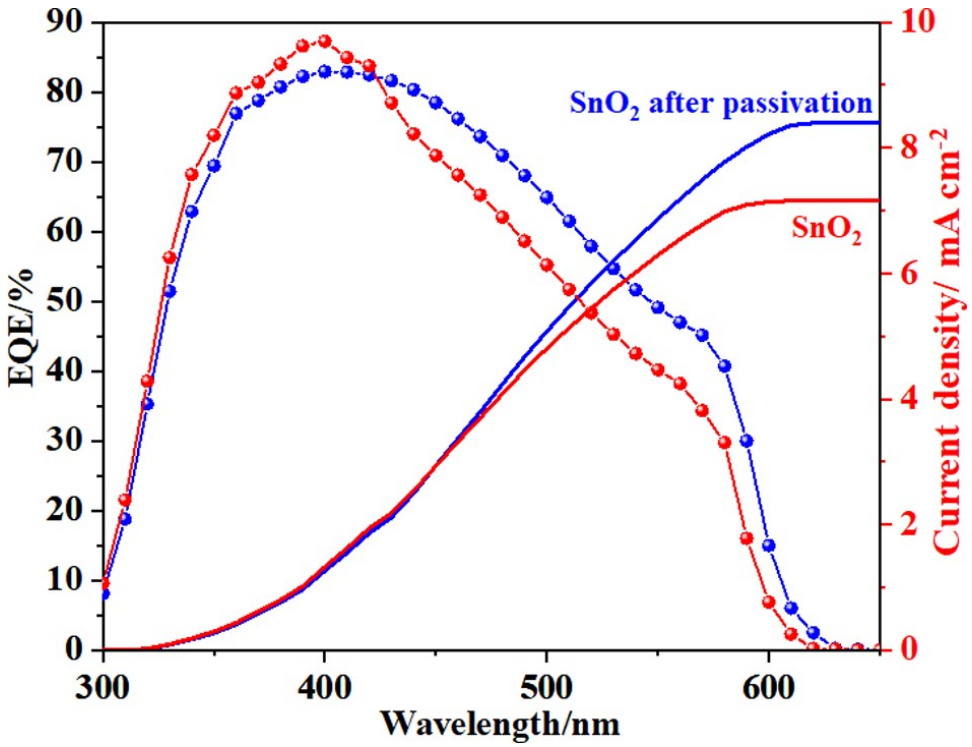

Figure S7 IPCE spectra of $CsPbIBr_2$ PSCs based on bare or passivated SnO_2 ESL.

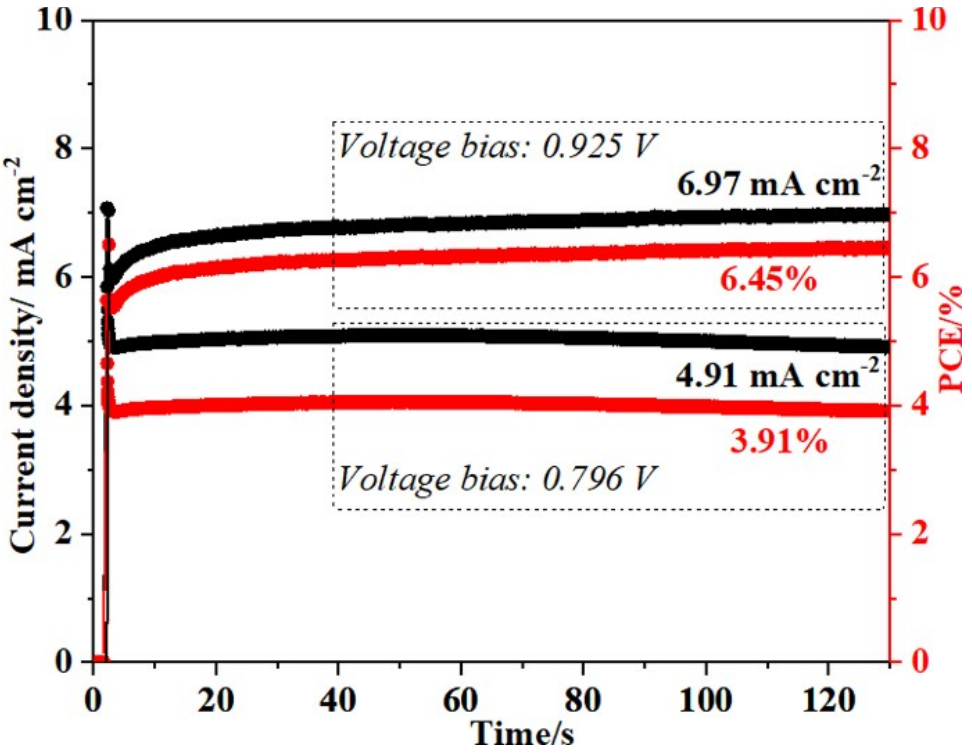

Figure S8 Stability of output of $CsPbIBr_2$ PSCs based on bare or passivated SnO_2 ESL.

Table S1 Summary of V_{oc} and PCE values for reported $CsPbIBr_2$-based solar cells under reverse scanning direction.

Method	Temperature/^{o}C	Device structure	Champion V_{oc}/V	Champion PCE/%	Ref.
One-step spin-coating	160	FTO/SnO_2/$CsPbIBr_2$/Carbon	**1.31**	7.00	This work
Spray-Assisted Deposition	300	FTO/c-TiO_2/m-TiO_2/$CsPbIBr_2$/Spiro-OMeTAD/Au	**1.13**	6.30	1
Thermal Evaporation	250	FTO/c-TiO_2/$CsPbIBr_2$/Au	**0.96**	4.70	2
Two-step dipping	135	FTO/NiO_x/$CsPbIBr_2$/ZnO/Al	**1.01**	5.57	3
Two-step dipping	350	FTO/c-TiO_2/m-TiO_2/$CsPbIBr_2$/Carbon	**0.96**	6.14	4
Two-step dipping	350	FTO/c-TiO_2/m-TiO_2/$CsPbIBr_2$/Carbon	**1.08**	8.25	5
One-step spin-coating	320	FTO/c-TiO_2/$CsPbIBr_2$/Spiro-OMeTAD/Au	**1.23**	8.02	6
One-step spin-coating	160	FTO/NiO_x/$CsPbIBr_2$/MoO_x/Au	**0.85**	5.52	7
One-step spin-coating	100	FTO/c-TiO_2/$CsPbIBr_2$/Carbon	**1.14**	6.55	8
One-step spin-coating	150	FTO/SnO_2/C60/$CsPbIBr_2$/Spiro-OMeTAD/Au	**1.18**	7.34	9
One-step spin-coating	280	FTO/c-TiO_2/$CsPbIBr_2$/Carbon	**1.245**	9.16	10

Table S2 Performances of 20 devices based on bare or passivated SnO_2 ESL under reverse scanning direction.

Bare SnO_2					Passivated SnO_2				
Sample No.	**V_{oc}(V)**	**J_{sc}(mA/cm^2)**	**FF**	**Eff/%**	**Sample No.**	**V_{oc}(V)**	**J_{sc}(mA/cm^2)**	**FF**	**Eff/%**
1	**1.07**	7.55	0.58	4.71	21	**1.23**	8.50	0.67	7.00
2	**1.07**	7.57	0.52	4.21	22	**1.22**	8.61	0.66	6.95
3	**1.06**	7.58	0.52	4.14	23	**1.22**	8.66	0.65	6.87
4	**1.01**	8.07	0.51	4.13	24	**1.22**	8.64	0.65	6.87
5	**1.06**	7.59	0.51	4.10	25	**1.21**	8.80	0.63	6.72
6	**1.01**	7.51	0.54	4.07	26	**1.21**	8.60	0.64	6.62
7	**1.00**	8.07	0.50	4.07	27	**1.22**	8.62	0.63	6.61
8	**0.99**	8.09	0.50	4.03	28	**1.22**	8.39	0.65	6.61
9	**1.03**	7.53	0.51	3.99	29	**1.21**	8.49	0.63	6.46
10	**1.03**	7.55	0.50	3.89	30	**1.22**	8.70	0.62	6.58
11	**1.02**	7.92	0.48	3.88	31	**1.22**	8.36	0.61	6.24
12	**0.98**	7.96	0.48	3.76	32	**1.20**	8.18	0.63	6.21
13	**0.91**	7.48	0.50	3.42	33	**1.22**	7.51	0.62	5.68
14	**0.95**	7.04	0.50	3.35	34	**1.25**	7.43	0.60	5.59
15	**0.94**	7.09	0.49	3.27	35	**1.23**	7.44	0.61	5.55
16	**0.89**	7.65	0.43	2.93	36	**1.22**	7.45	0.58	5.27
17	**0.88**	7.71	0.42	2.86	37	**1.27**	6.87	0.44	3.87
18	**0.89**	7.38	0.41	2.73	38	**1.26**	6.29	0.38	3.01
19	**0.89**	7.34	0.41	2.71	39	**1.31**	6.86	0.33	3.00
20	**0.85**	7.71	0.40	2.63	40	**1.31**	5.70	0.28	2.06

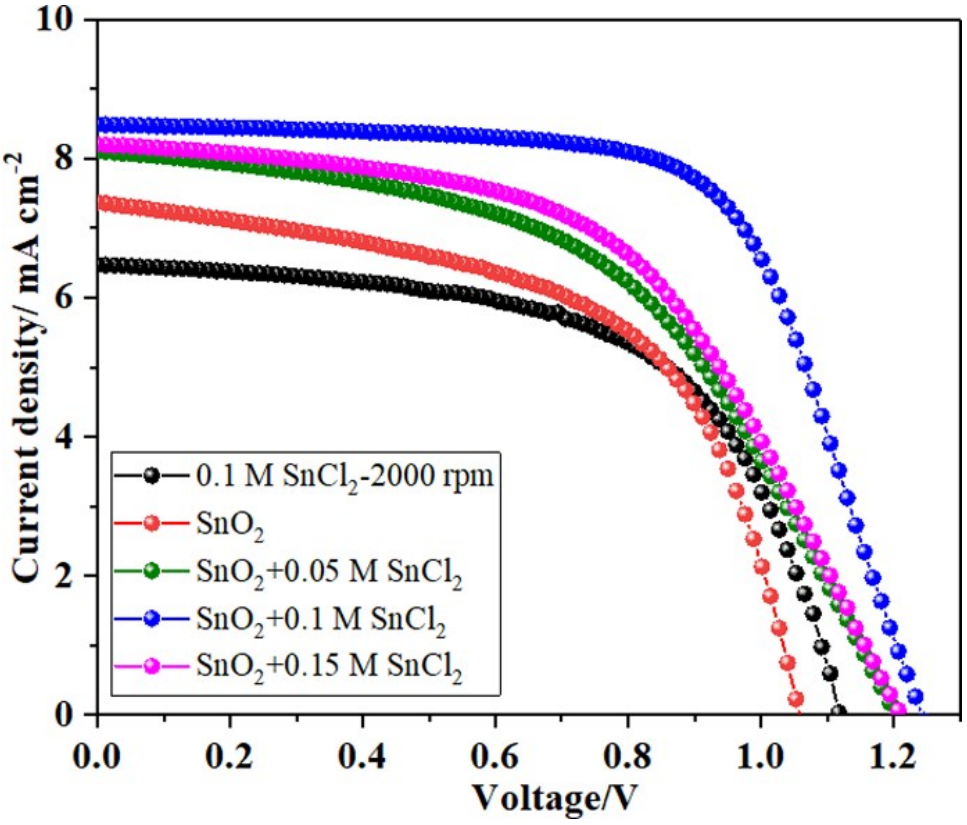

Figure S9 *J-V* curves of the PSCs based on different SnO_2 ESLs.

Table S3 Photovoltaic parameters of PSCs based on different SnO_2 ESLs.

	V_{oc}(V)	J_{sc}(mA/cm^2)	FF	Eff/%
0.1 M $SnCl_2$-2000 rpm	1.12	6.47	0.59	4.30
SnO_2	1.07	7.55	0.58	4.71
SnO_2+0.05 M $SnCl_2$	1.19	8.11	0.51	4.97
SnO_2+0.1 M $SnCl_2$	1.23	8.50	0.67	7.00
SnO_2+0.15 M $SnCl_2$	1.21	8.20	0.53	5.29

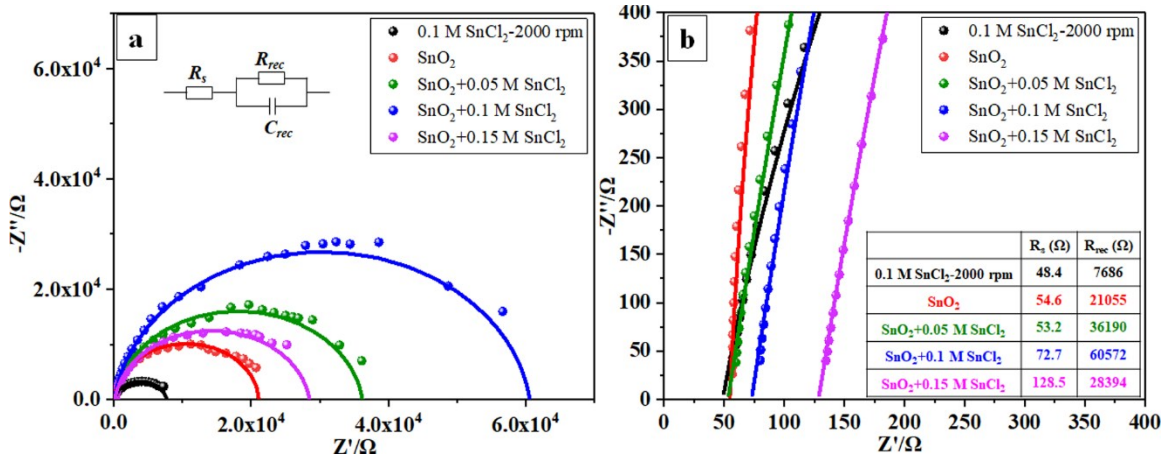

Figure S10 (a) Nyquist plots and (b) enlarged high-frequency region of PSCs different SnO_2 ESLs in dark condition at a voltage of V_{oc}. Inset: the equivalent circuit and table of simulated results.

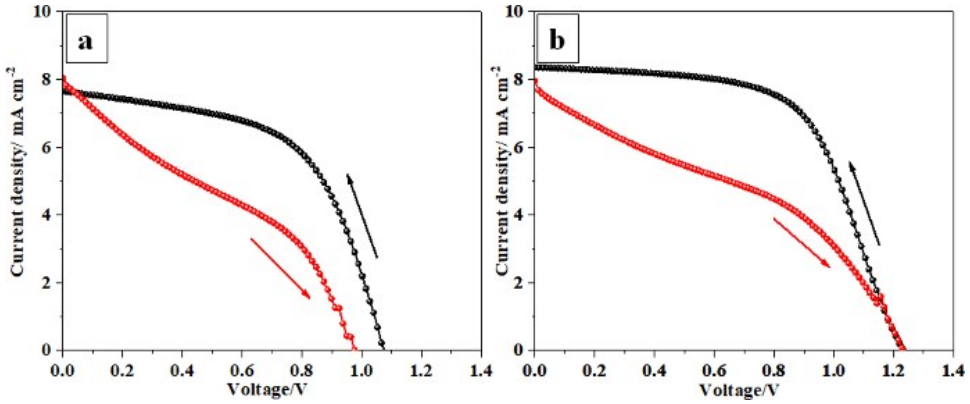

Figure S11 J-V curves with the reverse and forward scanning direction for the PSCs based on (a) bare and (b) passivated SnO_2 ESL.

Table S4 Photovoltaic parameters of J-V curves with the reverse and forward scanning direction for the PSCs based on bare and passivated SnO_2 ESL.

ESL	Scanning direction	V_{oc}(V)	J_{sc}(mA/cm^2)	FF	Eff/%	Hysteresis Index
SnO_2	Forward	0.98	8.04	0.34	2.66	43.0%
	Reverse	1.07	7.65	0.57	4.67	
Passivated SnO_2	Forward	1.23	7.96	0.37	3.60	42.3%
	Reverse	1.22	8.36	0.61	6.24	

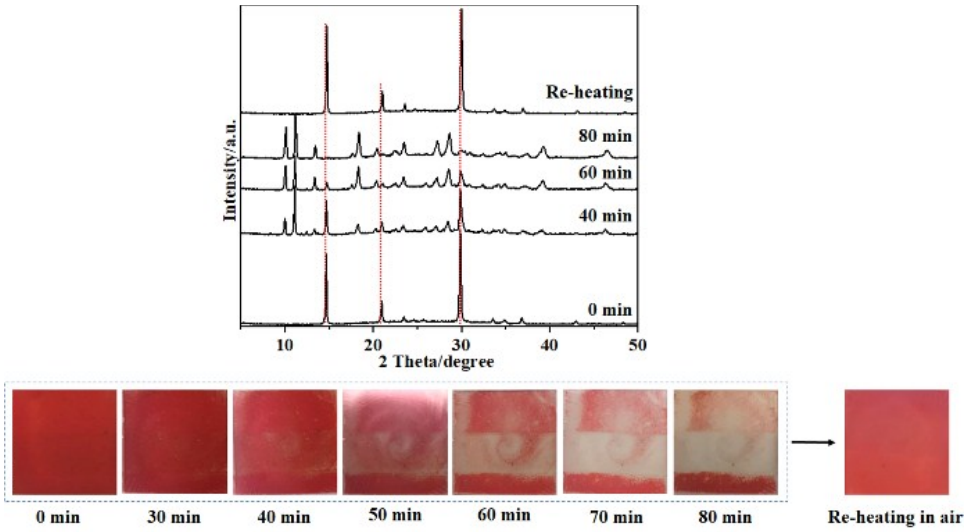

Figure S12 Time-dependent XRD patterns and photographs of the passivated SnO_2 based $CsPbIBr_2$ film when exposed to air at 25 °C with the humidity of 65%.

References

1. C. F. J. Lau, X. Deng, Q. Ma, J. Zheng, J. S. Yun, M. A. Green, S. Huang and A. W. Ho-Baillie, *ACS Energy Lett.*, 2016, **1**, 573.
2. Q. Ma, S. Huang, X. Wen, M. A. Green and A. W. Ho-Baillie, *Adv. Energy Mater.*, 2016, **6**, 1502202.
3. J. Lin, M. Lai, L. Dou, C. S. Kley, H. Chen, F. Peng, J. Sun, D. Lu, S. A. Hawks and C. Xie, *Nat. Mater.*, 2018, **17**, 261.
4. J. Liang, Z. Liu, L. Qiu, Z. Hawash, L. Meng, Z. Wu, Y. Jiang, L. K. Ono and Y. Qi, *Adv. Energy Mater.*, 2018, 1800504.
5. J. Liang, P. Zhao, C. Wang, Y. Wang, Y. Hu, G. Zhu, L. Ma, J. Liu and Z. Jin, *J. Am. Chem. Soc.*, 2017, **139**, 14009.
6. W. Li, M. U. Rothmann, A. Liu, Z. Wang, Y. Zhang, A. R. Pascoe, J. Lu, L. Jiang, Y. Chen and F. Huang, *Adv. Energy Mater.*, 2017, **7**, 1700946.
7. C. Liu, W. Li, J. Chen, J. Fan, Y. Mai and R. E. Schropp, *Nano Energy*, 2017, **41**, 75.
8. W. Zhu, Q. Zhang, C. Zhang, Z. Zhang, D. Chen, Z. Lin, J. Chang, J. Zhang and Y. Hao, *ACS Appl. Energy Mater.*, 2018.
9. N. Li, Z. Zhu, J. Li, A. K. Y. Jen and L. Wang, *Adv. Energy Mater.*, 2018, 1800525.
10. W. Zhu, Q. Zhang, D. Chen, Z. Zhang, Z. Lin, J. Chang, J. Zhang, C. Zhang and Y. Hao, *Adv. Energy Mater.*, 2018, 1802080.